

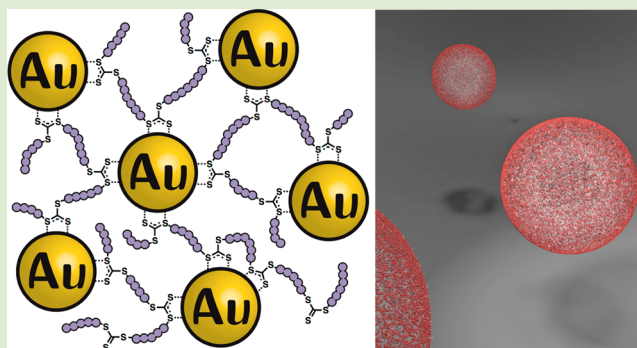
# Spherical Gold-Nanoparticle Assemblies with Tunable Interparticle Distances Mediated by Multifunctional RAFT Polymers

Christian Rossner, Bastian Ebeling, and Philipp Vana\*

Institut für Physikalische Chemie, Georg-August-Universität Göttingen, Tammannstraße 6, D-37077 Göttingen, Germany

**S** Supporting Information

**ABSTRACT:** A strategy for the controlled assembly of gold nanocrystals into dispersed three-dimensional superstructures is presented. A multifunctional RAFT agent was used to prepare multiblock polystyrene (4.4–17.8 kDa) with trithiocarbonate groups as junctions between the individual blocks. Addition of these polymers to two-phase Brust–Schiffrin gold nanoparticles (4.1 nm) resulted in the formation of stable gold-nanoparticle assemblies dispersed in toluene. TEM analysis revealed that the interparticle distances in these superstructures can be tuned over an unprecedented wide range by employing multiblock polymers with an adjusted degree of polymerization and thus tailored trithiocarbonate distances. Cross-linking of the gold nanoparticles in the assemblies by multifunctional trithiocarbonates was proven by AFM showing partly preserved globular shape after deposition on a solid substrate. The reported strategy is expected to prove useful when interparticle distances in nanoparticle assemblies need to be tuned in a liquid phase or on surfaces.



In recent years, colloidal superparticles<sup>1</sup> attracted growing attention due to potential applications ranging from but not limited to sensing,<sup>2</sup> photothermal therapy,<sup>3</sup> and surface-enhanced Raman spectroscopy.<sup>4</sup> One of the central requirements for the design and understanding of such particle assemblies is the ability to control the spatial arrangement of the individual particles.<sup>5–7</sup>

Due to the chemical stability and facile surface modification of gold nanoparticles (AuNPs), their spherical assemblies in particular are regarded as canonical model superstructures and are explored extensively.<sup>5,7–16</sup> Their formation is driven through cross-linking of individual particles mediated by a variety of distinct interactions, such as salt bridges,<sup>5</sup> hydrogen bonding,<sup>8,9,16</sup>  $\pi$ - $\pi$ -interactions,<sup>11</sup> metal coordination,<sup>13</sup> dipole-dipole-interactions,<sup>14</sup> halogen bonding,<sup>15</sup> and thiol-gold<sup>12</sup> and thioether-gold interactions.<sup>7,10</sup> The cross-linking species can take the form of dendrimers,<sup>5</sup> small molecules,<sup>7,10–15</sup> DNA,<sup>8</sup> polypeptides,<sup>16</sup> and synthetic polymers.<sup>9</sup> Because small molecules as cross-linking agents suffer from their inherent limitations,<sup>17</sup> polymers are attractive candidates for fulfilling the dual function of (1) providing good particle/assembly dispersion through steric stabilization and (2) directing self-assembly. Moreover, because there are tools available to control complex macromolecular architectures (like reversible-deactivation radical polymerization (RDRP) techniques), it can be envisaged to translate the macromolecular design to the structure of nanoparticle assemblies.<sup>18</sup>

Of all RDRP techniques, RAFT polymerization<sup>19</sup> is an attractive means of polymer fabrication in the context of gold nanoparticle chemistry, because RAFT polymers inherently

contain the thiocarbonylthio moiety, which can be used as an anchoring group for the attachment to gold surfaces.<sup>20</sup> Our lab recently examined in detail a strategy to prepare multiblock (co)polymers with trithiocarbonate (TTC) groups incorporated along their backbone<sup>21</sup> and we could show theoretically that the ideal distribution of TTC groups among the thus produced macromolecules is remarkably narrow.<sup>22</sup> It is known that RAFT polymers bind to gold nanoparticles with their TTC groups, be they in the middle<sup>23</sup> or at the  $\omega$ -end<sup>24</sup> of the polymeric chain, and multifunctional RAFT polymers can therefore be considered as potential cross-linkers for AuNPs. This in mind, we evaluated the binding mode of these multifunctional RAFT polymers with AuNPs from citrate reduction in a preceding study,<sup>25</sup> in which no particle cross-linking was observed and all particles were well isolated. As a matter of fact, however, AuNPs can assemble or not when treated with a cross-linking agent, depending on their properties, which stem from the preparation protocol used.<sup>26</sup> We, therefore, intended to expand our investigations to two-phase Brust–Schiffrin AuNPs and report first results here.

Two RAFT agents were used in this study (Figure 1) and their interaction with tetraoctylammonium-bromide(TOAB)-capped AuNPs was evaluated. The RAFT agent 2, containing  $N_{TTC}$  TTC groups, was synthesized in a polycondensation reaction, as described in our previous publications.<sup>21,25</sup> RAFT

**Received:** October 30, 2013

**Accepted:** November 21, 2013

**Published:** November 25, 2013

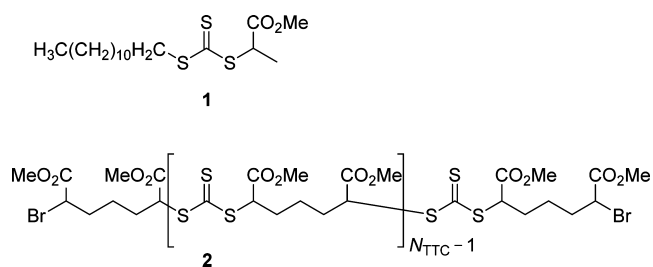


**Figure 1.** RAFT agents used in this study with a single **1** and multiple TTC moieties **2**.

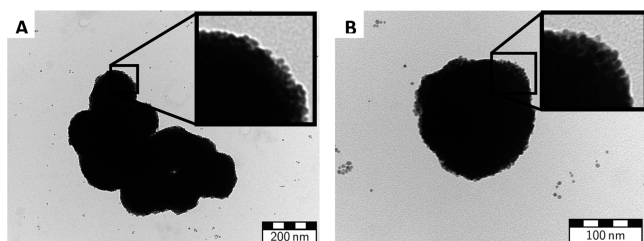


**Figure 2.** Representative TEM images of AuNPs treated with RAFT agent **2**, without inserted monomer. Large particle agglomerates (**A**) and spherical particle assemblies (**B**) were found. Magnified details (shown as insets in images **A** and **B**) unequivocally prove that these structures are composed of AuNPs as building units.

**Table 1.** Results from Analysis of the Multiblock Polymers

multiblock polymer	DP <sub>NMR</sub>	M <sub>n,SEC,RI</sub> (g × mol <sup>-1</sup> )	D <sub>SEC,RI</sub>	N <sub>TTC</sub>
I	4	4400	1.70	5.7
II	10	7900	1.89	5.7
III	27	17800	2.22	5.6

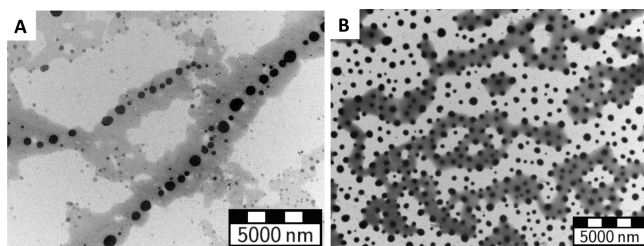


**Figure 3.** TEM images of nanohybrids of **I** (image **A**) and **III** (image **B**), taken at low magnification.

agent **1**, dodecyl 1-(methoxycarbonyl)ethyl trithiocarbonate, was synthesized by a standard method (SI, NMR data Figures S1 and S2) and served for reference as a structural analog of **2** with only one TTC group.

Compound **1** was designed to mirror the characteristics of **2**. At the same time, the long hydrocarbon chain in **1** was introduced in the Z group to make surface modification of AuNPs possible, since stabilization of colloidal particles almost certainly fails if the protecting ligand shell becomes too thin.<sup>27</sup>

Both RAFT agents were added to toluene dispersions of TOAB-stabilized AuNPs that had been prepared by the two-phase Brust–Schiffirin synthesis (see SI). Because TOAB is only weakly chemisorbed on their surfaces,<sup>28</sup> such particles can be used as a platform for ligand exchange reactions.<sup>29</sup> These reactions were undertaken by adding a solution of the respective RAFT agent in toluene to the AuNP dispersion under ultrasonication (see SI). In the case of RAFT agent **1**, a

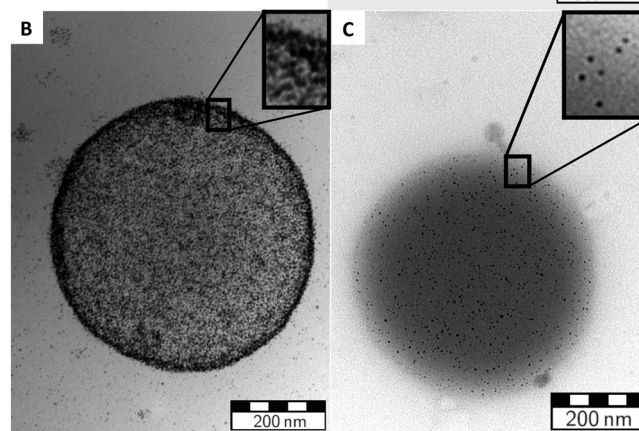
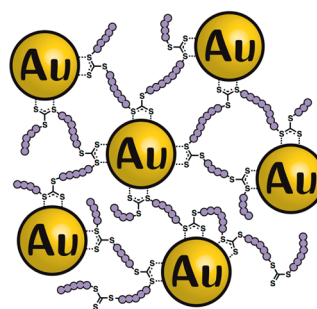


**Figure 4.** Schematic representation of the binding mode (upper left) and TEM images of spherical assemblies of AuNPs cross-linked with multiblock polymers **I**, **II**, and **III** (images **A**, **B**, and **C**, respectively).

ruby-red dispersion was obtained and the visible spectrum revealed a relatively narrow absorbance band centered at 520 nm, indicative of well-separated individual AuNPs (Figure S3a). The nanoparticles modified with RAFT agent **1** displayed excellent colloidal stability: Dispersions could be stored at ambient conditions over several weeks, and the modified particles can be dried and redispersed after four months without losing their integrity, showing the high performance of this kind of ligand to shield the AuNP surface. In marked contrast, a black precipitate settled to the bottom of the tube when AuNPs were treated with **2**. Precipitation was not quantitative because the red color of the supernatant sustained, indicating remaining AuNPs present in the dispersion. The precipitate was redispersed in DMF, resulting in a blue-transmitting dispersion, from which a black precipitate settled again within 1 h, showing the poor colloidal stability of the nanocomposites of **2**. Visible spectroscopy (Figure S3b) revealed a broadened and red-shifted absorbance band at 700 nm and reduced transmittance at all wavelengths in the range investigated, when compared with the spectrum in Figure S3a. Both observations are consistent with the formation of large AuNP assemblies, which will cause light scattering and a surface plasmon resonance band red-shift, due to dipolar couplings of neighboring AuNPs.<sup>30</sup>

To verify these hypotheses, developed based on visible spectroscopy data, transmission electron microscopy (TEM) visualization of the gold–polystyrene nanohybrids was undertaken. As expected, AuNPs treated with **1** appeared as individual particles; absolutely no particle coalescence or

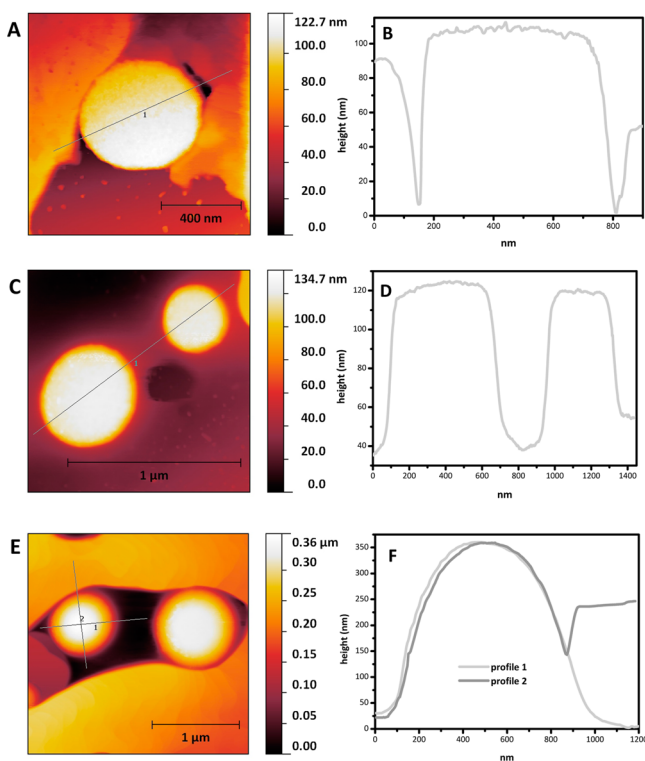


**Figure 5.** AFM images of spherical assemblies found for AuNPs cross-linked with multiblock polymers **I**, **II**, and **III** (images A, C, and E, respectively). Cross-sectional profiles are shown in the plots labeled B, D, and F.

twinning was observed. The AuNPs arranged into a two-dimensional hexagonal pattern, as described previously (Figure S4).<sup>25</sup> This sample was also used to determine the size-distribution of the AuNPs prepared by the protocol used here (diameter histogram in Figure S5).<sup>25</sup> A mean particle diameter of  $(4.1 \pm 0.9)$  nm was obtained. TEM inspection of particles treated with **2** revealed larger AuNP assemblies (Figure 2), as already anticipated from visible spectroscopy.

The vast majority of AuNPs visualized by means of TEM were located in very large particle assemblies (in the  $\mu\text{m}$  size regime, see Figure S6 for an overview micrograph) of irregular shape (image A in Figure 2). A closer look at those assemblies, however, shows that they can be thought of being made from smaller, spherical particle assemblies. If this is true, then some of those spherical subunits, which not yet have assembled into larger secondary structures, should also be present. As micrograph B shows, this is in fact the case. It can be concluded that particle cross-linking by the multifunctional TTC (RAFT agent **2**) induces formation of spherical AuNP assemblies. The organic layer exposed on the surface of those assemblies, however, appears to provide not enough stabilization in the respective solvent, such that agglomeration into larger secondary structures ensues.

We were next interested if the spherical AuNP assemblies can be prevented from agglomeration into ill-defined secondary structures, as seen in Figure 2, when polymers derived from RAFT agent **2** are used as cross-linking agents. For this purpose, styrene represents an ideal candidate of monomer since (1) its polymerization can be achieved with good control over the overall process with the respective RAFT agent **2**;<sup>21</sup> (2) the introduction of styrene units is expected to provide solubility to the multiblock polymers in toluene, which may

result in steric stabilization of their nanocomposites; (3) if desired, multiblock copolymers with acrylates and acrylamides are readily accessible through a second RAFT polymerization, when polystyrene is used as the first block; and (4) polystyrene is expected to give a higher contrast in TEM than other polymers, due to electron interaction with the aromatic systems, making its visualization possible.<sup>31</sup> Furthermore, (5) it had already been shown that styrene oligomers with a very short chain length (two styrene units) can be prepared when a TTC chain transfer agent with a 2-propionate R group is used,<sup>32</sup> which is comparable to the leaving group in the system presented herein. It should, therefore, be possible to vary the degree of polymerization (DP) and along with that the TTC-group distances in one macromolecule in a wide range from very short spacings, when a low degree of polymerization is targeted, to larger distances with increasing DP. (Herein, we like to refer to DP as the number of monomer units per TTC group.) The multiblock polymers obtained were characterized by a combination of  $^1\text{H}$  NMR spectroscopy (Figure S8) and SEC (Figure S9; full description of the analysis is provided in SI). The results of the analyses (i.e., along with DP and  $N_{\text{TTC}}$ , the average molecular weight,  $M_n$ , and dispersity,  $D$ , of the multiblock polymers) are given in Table 1.

All polymers **I–III** were added to TOAB-stabilized AuNPs in a molar ratio of approx. 570 macromolecules per particle. Unlike with the pure RAFT agent **2** without inserted monomer, in none of the three cases a precipitate formed here. All dispersions were ruby-red (one visible spectrum is exemplarily shown in Figure S10). For the nanohybrids of **I** and **III**, where the DP of styrene is lowest and highest, respectively, TEM images are shown at low magnifications in Figure 3.

Deposited polystyrene can be seen in both micrographs in Figure 3 (gray area) together with several isolated spheres (black). The spheres are sometimes colocalized with polystyrene but can be found in regions where no or less polymer is deposited as well. The average diameter of the spherical objects is orders of magnitude higher than that of the individual AuNPs and was determined to be  $(3.5 \pm 3.3) \times 10^2$  nm for nanohybrids of **I**,  $(3.9 \pm 3.3) \times 10^2$  nm for nanohybrids of **II**, and  $(4.1 \pm 1.5) \times 10^2$  nm for nanohybrids of **III** (based on the analysis of 1409, 1912, and 1423 spheres found on 11, 11, and 5 individual images, respectively). These relatively broad size distributions are indeed typical for superparticles made from nanoparticle assembly.<sup>1</sup> From images of isolated spheres taken at higher magnifications (Figure 4), it can be concluded that they are composed of individual nanoparticles, which are most likely cross-linked by polymer “mortar”. The interparticle distances in those spherical assemblies are correlated to the DP of the cross-linking multiblock polymers. Figure 4C, which shows an assembly with the largest particle–particle separations, shows that AuNPs within the assembly can be regarded as individual units that do not fuse into larger aggregates.

The spherical assemblies were also characterized by AFM to ascertain their three-dimensional shape (Figure 5). If assemblies preserve a globular structure after drop-casting on a solid substrate and solvent evaporation, this can be regarded as an indication for particle cross-linking, since neighboring particles are prevented from shear-slipping when bonded together.<sup>33</sup> The AFM images also show objects with spherical outlines. The obtained height profiles reveal that the spherical assemblies do not smear out to flat circular disks, but rather partly preserve their globular shape, which proves particle cross-linking. It is interesting to note the object surface becoming more and more

smooth with increasing DP of styrene (rough surface in height profile labeled B and smooth surface in height profile labeled F). This behavior can be explained by more effective shielding of individual AuNPs on the superparticles' surfaces, when the polystyrene ligand becomes larger.

In summary, we found that multifunctional RAFT polymers can be used to assemble Brust–Schiffrin AuNPs into spherical superstructures. This represents, to the best of our knowledge, the first report of AuNP network formation through cross-linking with multifunctional TTCs. The AuNP interparticle distances were shown to be easily tunable over an unprecedented wide range by adjusting the DP of the polymer “mortar” in a single polymerization. This useful feature unburdens from the necessity of multistep organic synthesis to define the AuNP linker length and offers a more straightforward and efficient approach for the synthesis of gold superparticles with defined spatial organization of the individual nanoparticles. The concept was demonstrated using polystyrene, but should in principle be applicable to various other (co)polymers, which at the same time renders this system very versatile since linker length can be tuned without a need to modify the desired chemical composition of the “mortar”.

## ■ ASSOCIATED CONTENT

### ■ Supporting Information

Synthetic procedures, NMR spectra, SEC traces of the employed multiblock polymers, more information on the used AuNPs, and additional transmission electron micrographs. This material is available free of charge via the Internet at <http://pubs.acs.org>.

## ■ AUTHOR INFORMATION

### ■ Corresponding Author

\*E-mail: [pvana@uni-goettingen.de](mailto:pvana@uni-goettingen.de).

### ■ Notes

The authors declare no competing financial interest.

## ■ ACKNOWLEDGMENTS

Financial support by the Deutsche Forschungsgemeinschaft (Project No. VA226/4-2) is gratefully acknowledged. We are thankful to Dr. Jens Grosche, Effigos AG Leipzig, Germany, for designing the table of contents artwork. C.R. acknowledges a scholarship of the Studienstiftung des deutschen Volkes. P.V. acknowledges receipt of a Heisenberg-Professorship (DFG).

## ■ REFERENCES

- (1) Wang, T.; LaMontagne, D.; Lynch, J.; Zhuang, J.; Cao, Y. C. *Chem. Soc. Rev.* **2013**, *42*, 2804–2823.
- (2) Elghanian, R.; Storhoff, J. J.; Mucic, R. C.; Letsinger, R. L.; Mirkin, C. A. *Science* **1997**, *277*, 1078–1081.
- (3) Nam, J.; La, W.-G.; Hwang, S.; Ha, Y. S.; Park, N.; Won, N.; Jung, S.; Bhang, S. H.; Ma, Y.-J.; Cho, Y.-M.; Jin, M.; Han, J.; Shin, J.-Y.; Wang, E. K.; Kim, S. G.; Cho, S.-H.; Yoo, J.; Kim, B.-S.; Kim, S. *ACS Nano* **2013**, *7*, 3388–3402.
- (4) Hao, E.; Schatz, G. C. *J. Chem. Phys.* **2004**, *120*, 357–366.
- (5) Frankamp, B. L.; Boal, A. K.; Rotello, V. M. *J. Am. Chem. Soc.* **2002**, *124*, 15146–15147.
- (6) DeVries, G. A.; Brunnbauer, M.; Hu, Y.; Jackson, A. M.; Long, B.; Neltner, B. T.; Uzun, O.; Wunsch, B. H.; Stellacci, F. *Science* **2007**, *315*, 358–361.
- (7) Lim, I.-I. S.; Vaiana, C.; Zhang, Z.-Y.; Zhang, Y.-J.; An, D.-L.; Zhong, C.-J. *J. Am. Chem. Soc.* **2007**, *129*, 5368–5369.
- (8) Mirkin, C. A.; Letsinger, R. L.; Mucic, R. C.; Storhoff, J. J. *Nature* **1996**, *382*, 607–609.

- (9) Boal, A. K.; Ilhan, F.; DeRouchey, J. E.; Thurn-Albrecht, T.; Russel, T. P.; Rotello, V. M. *Nature* **2000**, *404*, 746–748.
- (10) Maye, M. M.; Lim, I.-I. S.; Luo, J.; Rab, Z.; Rabinovich, D.; Liu, T.; Zhong, C.-J. *J. Am. Chem. Soc.* **2005**, *127*, 1519–1529.
- (11) van Herrikhuyzen, J.; Janssen, R. A. J.; Meijer, E. W.; Meskers, S. C. J.; Schenning, A. P. H. J. *J. Am. Chem. Soc.* **2006**, *128*, 686–687.
- (12) Hussain, I.; Wang, Z.; Cooper, A. I.; Brust, M. *Langmuir* **2006**, *22*, 2938–2941.
- (13) Zhang, X.; Li, D.; Zhou, X.-P. *New J. Chem.* **2006**, *30*, 706–711.
- (14) Klajn, R.; Bishop, K. J. M.; Grzybowski, B. A. *Proc. Natl. Acad. Sci. U.S.A.* **2007**, *104*, 10305–10309.
- (15) Shirman, T.; Arad, T.; van der Boom, M. E. *Angew. Chem., Int. Ed.* **2010**, *49*, 926–929.
- (16) Wang, J.; Xia, H.; Zhang, Y.; Lu, H.; Kamat, R.; Dobrynin, A. V.; Cheng, J.; Lin, Y. *J. Am. Chem. Soc.* **2013**, *135*, 11417–11420.
- (17) Grzelczak, M.; Vermant, J.; Furst, E. M.; Liz-Marzán, L. M. *ACS Nano* **2010**, *4*, 3591–3605.
- (18) Celiz, A. D.; Lee, T.-C.; Sherman, O. A. *Adv. Mater.* **2009**, *21*, 3937–3940.
- (19) Chiefari, J.; Chong, Y. K.; Ercole, F.; Krstina, J.; Jeffery, J.; Le, T. P. T.; Mayadunne, R. T. A.; Meijs, G. F.; Moad, C. L.; Moad, G.; Rizzardo, E.; Thang, S. H. *Macromolecules* **1998**, *31*, 5559–5562.
- (20) Duwez, A.-S.; Guillet, P.; Colard, C.; Gohy, J.-F.; Fustin, C.-A. *Macromolecules* **2006**, *39*, 2729–2731.
- (21) Ebeling, B.; Vana, P. *Polymers* **2011**, *3*, 719–739.
- (22) Ebeling, B.; Eggers, M.; Vana, P. *Macromolecules* **2010**, *43*, 10283–10290.
- (23) Fustin, C.-A.; Colard, C.; Filali, M.; Guillet, P.; Duwez, A.-S.; Meier, M. A. R.; Schubert, U. S.; Gohy, J.-F. *Langmuir* **2006**, *22*, 6690–6695.
- (24) Boyer, C.; Whittaker, M. R.; Nouvel, C.; Davis, T. P. *Macromolecules* **2010**, *43*, 1792–1799.
- (25) Ebeling, B.; Vana, P. *Macromolecules* **2013**, *46*, 4862–4871.
- (26) Hussain, I.; Brust, M.; Barauskas, J.; Cooper, A. I. *Langmuir* **2009**, *25*, 1934–1939.
- (27) Korgel, B. A.; Fullam, S.; Connolly, S.; Fitzmaurice, D. *J. Phys. Chem. B* **1998**, *102*, 8379–8388.
- (28) Fink, J.; Kiely, C. J.; Bethell, D.; Schiffrin, D. J. *Chem. Mater.* **1998**, *10*, 922–926.
- (29) Zhou, J.; Beattie, D. A.; Sedev, R.; Ralston, J. *Langmuir* **2007**, *23*, 9170–9177.
- (30) Storhoff, J. J.; Lazarides, A. A.; Mucic, R. C.; Mirkin, C. A.; Letsinger, R. L.; Schatz, G. C. *J. Am. Chem. Soc.* **2000**, *122*, 4640–4650.
- (31) Moraes, J.; Ohno, K.; Gody, G.; Maschmeyer, T.; Perrier, S. *Beilstein J. Org. Chem.* **2013**, *9*, 1226–1234.
- (32) Siau, M.; Hawke, B. S.; Perrier, S. *J. Polym. Sci., Part A: Polym. Chem.* **2012**, *50*, 187–198.
- (33) Lin, G.; Wang, Y.; Zhang, Q.; Zhang, X.; Ji, G.; Ba, L. *Nanoscale* **2011**, *3*, 4567–4570.